Semiconductor saturable-absorber mirror–assisted Kerr-lens mode-locked Ti:sapphire laser producing pulses in the two-cycle regime

D. H. Sutter, G. Steinmeyer, L. Gallmann, N. Matuschek, F. Morier-Genoud, and U. Keller

Ultrafast Laser Physics Laboratory, Institute of Quantum Electronics, Swiss Federal Institute of Technology, ETH Hönggerberg–HPT, CH-8093 Zürich, Switzerland

V. Scheuer, G. Angelow, and T. Tschudi

Institute for Applied Physics, Hochschulstrasse 6, D-64829 Darmstadt, Germany

Received December 21, 1999

Pulses of sub-6-fs duration have been obtained from a Kerr-lens mode-locked Ti:sapphire laser at a repetition rate of 100 MHz and an average power of 300 mW. Fitting an ideal sech^2 to the autocorrelation data yields a 4.8-fs pulse duration, whereas reconstruction of the pulse amplitude profile gives 5.8 fs. The pulse spectrum covers wavelengths from above 950 nm to below 630 nm, extending into the yellow beyond the gain bandwidth of Ti:sapphire. This improvement in bandwidth has been made possible by three key ingredients: carefully designed spectral shaping of the output coupling, better suppression of the dispersion oscillation of the double-chirped mirrors, and a novel broadband semiconductor saturable-absorber mirror. © 1999 Optical Society of America

OCIS codes: 320.7090, 320.0320, 320.5540, 140.3590.

Previously, to our knowledge the shortest pulses directly from a laser oscillator, with durations of 6.5 fs,[1] have been obtained from a Kerr-lens mode-locked Ti:sapphire laser with double-chirped mirrors (DCM's),[2] together with a prism pair for dispersion control. It has been shown that broadband semiconductor saturable-absorber mirrors[3] (SESAM's) provide a reliable mode-locking mechanism, with mode-locking buildup times down to 60 μs.[4] Moreover, SESAM-assisted Kerr-lens mode locking (KLM) relaxes the tight constraints on cavity alignment that are required for pure KLM.

In this Letter we demonstrate sub-6-fs pulses at an average output power of 300 mW (Fig. 1). The pulse spectrum covers wavelengths from above 950 nm to below 630 nm, with some clearly visible spectral content in the yellow. This extreme spectral width has been achieved by optimized spectral shaping of the output-coupling mirror (OC). The resonator is a standard 100-MHz X cavity with 10-cm-radius folding mirrors and a 2.3-mm Ti:sapphire crystal with 0.25-wt. % doping (see Fig. 2). Except for the OC, only broadband DCM's are used in the cavity, so the spectrum is not restricted by the limited bandwidth of standard femtosecond coatings. We have used either a novel ultrabroadband OC with a flat transmission curve or an OC designed specifically for spectral shaping. The DCM's, together with a pair of fused-silica Brewster prisms for adjustment, compensate for the intracavity dispersion. A new broadband SESAM is used to stabilize the Kerr-lens mode-locked operation over a broader range of cavity parameters.

The DCM's were fabricated with optically monitored ion-beam sputtering, and their dispersion was characterized by white-light interferometry. Unlike the DCM's used in the study reported in Ref. 4, we use improved coatings of broader bandwidth, based on both better growth control and an expanded analytical design theory.[5] However, the group-delay dispersion (GDD) of broadband DCM's generally oscillates around the target GDD. The combined action of GDD and self-phase modulation inside the cavity provides a mechanism for spectral energy transfer, concentrating energy spectrally at the minima of the intracavity GDD.[6] Comparison of the net cavity GDD [Fig. 3(b)] with the mode-locked spectrum

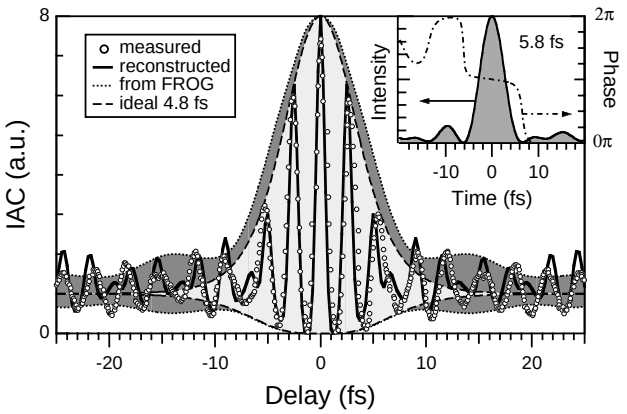

Fig. 1. Interferometric autocorrelation (IAC) measured and reconstructed with the algorithm described in Ref. 7, along with an IAC envelope reconstructed from a nondeconvolved frequency-resolved optical gating (FROG) measurement and an IAC envelope of an ideal 4.8-fs sech^2 pulse. Note that the trace reconstructed from the FROG data is 24% wider than the measured one, indicating a geometric blurring of the pulse duration of more than 1 fs. Inset: reconstructed pulse shape from IAC and spectrum.

0146-9592/99/090631-03$15.00/0

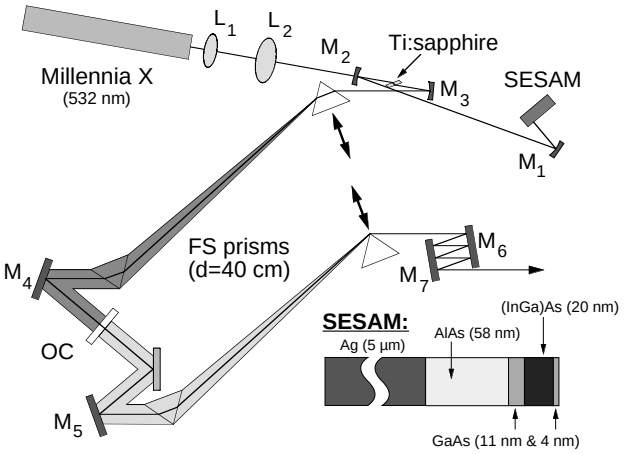

Fig. 2. Ti:sapphire laser resonator and extracavity dispersion-compensation setup: M1–M7, DCM's; FS prisms, fused-silica prisms with 40-cm apex separation; L's, lenses. Bottom right: detailed SESAM structure.

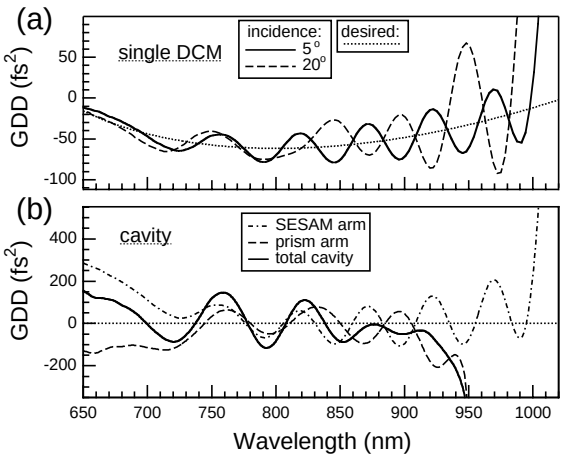

Fig. 3. GDD (a) desired and calculated for a single reflection on a DCM under 5° and 20° p-polarized incidence and (b) round trip through both resonator arms, separately and through the total cavity, as calculated from the measured GDD of the individual components.

(Fig. 4) confirms this trend. The four peaks of the power spectrum correspond to the minima of the overall GDD. The peaks in the spectrum become more pronounced with stronger GDD oscillation at long wavelengths. Ultimately, GDD poses a barrier at ~950 nm to further extension of the spectrum. To reduce detrimental GDD oscillations we carefully choose the incidence angle of folding mirror M4 to shift the GDD characteristics of the DCM coating [Fig. 3(a)]. Consequently, four DCM's can be combined without excessive GDD variation, allowing for extremely short pulses (in Refs. 1 and 4 only one and two DCM's, respectively, were used). The DCM's are placed in the cavity in such a way that the negative GDD is equally distributed on both sides of the Ti:sapphire crystal. This distribution allows the laser pulse to have the minimum chirp at both passes through the crystal, as well as at the OC and the SESAM.

The pulses are stabilized by a novel low-finesse antiresonant Fabry–Perot-type SESAM that consists of a silver bottom mirror, followed by a 58-nm-thick AlAs spacer layer and three absorbing layers: 11 nm of GaAs, 20 nm of $In_{0.22}Ga_{0.78}As$, and 4 nm of GaAs at the top (Fig. 2). The InGaAs quantum well provides absorption for wavelengths $\lambda < 1.05\ \mu$m, and the GaAs layers add absorption for $\lambda < 870$ nm; see Fig. 5. The modulation depth is $\Delta R \approx 4\%$ over a bandwidth of 400 nm, significantly broader than in Ref. 4. We measured a saturation fluence $F_{\mathrm{sat}} \approx 180\ \mu\mathrm{J/cm^2}$ and an absorber recovery time $\tau \approx 2.6$ ps because of carrier trapping and recombination. Unlike in pure KLM, the cavity alignment and the starting of the pulsed operation are significantly simplified by the SESAM. The laser runs for many hours with little change in power or pulse width. Moreover, KLM can be sustained over a relatively wide range of cavity parameters. This allows us to work in a region characterized by superior beam quality and higher average output power than with pure KLM without a SESAM.

We performed experiments with two custom-designed OC's, one with increased transmission in the spectral wings and an ultrabroadband OC with almost constant transmission from 650 nm to 1.1 μm (Fig. 5).

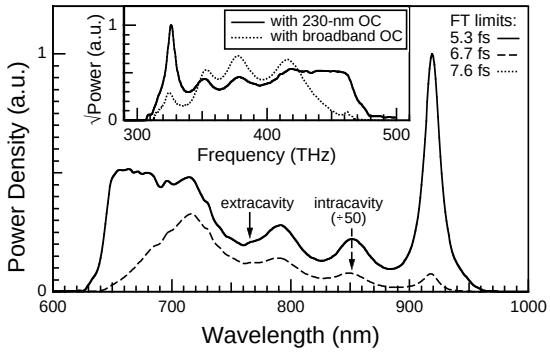

Fig. 4. Measured pulse spectrum obtained with a 230-nm bandwidth OC specifically designed for enhanced transmission in the wings of the spectrum, compared with the calculated intracavity spectrum. Inset: square root of the power density versus frequency obtained with the two OC's. The Fourier-transform-limited pulse durations for the three different spectra are given at the top right.

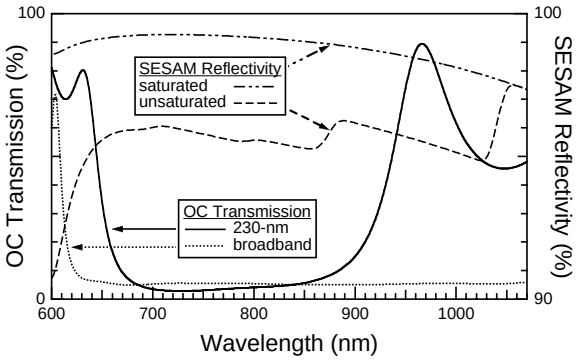

Fig. 5. Transmission of the OC used for the shortest pulses (230-nm bandwidth) and of the spectrally flat broadband 5% OC. Calculated SESAM reflectivity is shown for low-intensity light (unsaturated) and for high-intensity pulses (saturated).

Although both OC's produce essentially the same intracavity spectrum, spectral shaping of the output coupling allows for significant broadening of the extracavity spectrum without affecting the intracavity spectrum (Fig. 4).

So far, characterization of the shortest pulses has relied mainly on a sech^2 fit to the measured autocorrelation. Using a least-squares fit to the central part of the autocorrelation, shown in Fig. 1, we determine a 4.8-fs sech^2 pulse width. However, Fourier transformation of the spectrum yields a lower boundary of 5.3 fs for the pulse width. To achieve a more realistic estimate that is not biased by the choice of a particular pulse shape, we employ an iterative algorithm to reconstruct pulse amplitude and phase from both autocorrelation and spectrum.[7] This algorithm gives a pulse duration of 5.8 fs (inset of Fig. 1).

In addition, we use frequency-resolved optical gating[8] to characterize our pulses. Frequency-resolved optical gating also yields a 5.8-fs pulse, after correcting for the limited temporal resolution that is due to the noncollinear geometry.[9,10] We are forced to use a relative large crossing angle of 2.4° between the beams at a spot size of 55 μm to avoid interference. Assuming Gaussian spatiotemporal beam profiles, this leads to 1-fs blurring of the 5.8-fs pulse (see Fig. 1).

For most applications of ultrashort pulses, the exact pulse shape and duration are not a concern. Limitations arise owing to either autocorrelation width (e.g., in ultrafast pump–probe spectroscopy) or spectral width (e.g., in optical coherence tomography). In both these respects the pulses reported here are record breaking, with an autocorrelation width below three fringes (corresponding to a 4.8-fs sech^2 pulse) and a spectrum spanning more than 170 THz. These are the key numbers that should be used in comparing these results with previously published work, while the actual pulse width is 5.8 fs, as discussed above. To our knowledge, this result represents the shortest well-characterized pulses with the broadest bandwidth ever reported directly from a mode-locked laser. Shorter pulses have been generated extracavity at lower repetition rates only by nonlinear spectral broadening and subsequent compression.[10,11] Future efforts will concentrate on new DCM's and improved OC's that allow for less-modulated spectra of similar bandwidth.

As demonstrated in this Letter, spectral shaping of the output coupling can be used as a very efficient way to produce shorter pulses and to extend the spectrum of mode-locked pulses beyond the gain bandwidth. With the entire gain bandwidth of Ti:sapphire, an intracavity pulse of ≈5-fs duration can be generated. In this ultimate situation, similar spectral shaping would result in a sub-4-fs pulse width. This result clearly shows that, even with the sub-6-fs pulses reported in this Letter, there is still some potential for shorter pulses and that the ultimate limit for Ti:sapphire lasers has not yet been reached.

This work was supported by the Swiss National Science Foundation. D. H. Sutter's e-mail address is sutter@iqe.phys.ethz.ch.

Note added in proof: Recently, Morgner *et al.*[12] also obtained pulses in the two-cycle regime from a similar laser including DCM's but without a SESAM. While the FWHM of their IAC was slightly narrower, the larger wings indicate stronger energy content in prepulses and (or) postpulses.

We have recently obtained pulses with spectral bandwidths of 410 nm and a Fourier-transform limit of 4.9 fs. For these pulses, however, the measured IAC's indicate a larger residual chirp in the spectral wings, owing to stronger self-phase modulation in the laser crystal and to the limited bandwidth of the extracavity dispersion compensatin setup.

References

1. I. D. Jung, F. X. Kärtner, N. Matuschek, D. H. Sutter, F. Morier-Genoud, G. Zhang, U. Keller, V. Scheuer, M. Tilsch, and T. Tschudi, Opt. Lett. **22,** 1009 (1997).
2. F. X. Kärtner, N. Matuschek, T. Schibli, U. Keller, H. A. Haus, C. Heine, R. Morf, V. Scheuer, M. Tilsch, and T. Tschudi, Opt. Lett. **22,** 831 (1997).
3. I. D. Jung, F. X. Kärtner, N. Matuschek, D. H. Sutter, F. Morier-Genoud, Z. Shi, V. Scheuer, M. Tilsch, T. Tschudi, and U. Keller, Appl. Phys. B **65,** 137 (1997).
4. D. H. Sutter, I. D. Jung, F. X. Kärtner, N. Matuschek, F. Morier-Genoud, V. Scheuer, M. Tilsch, T. Tschudi, and U. Keller, IEEE J. Sel. Topics Quantum Electron. **4,** 169 (1998).
5. N. Matuschek, F. X. Kärtner, D. H. Sutter, V. Scheuer, M. Tilsch, T. Tschudi, and U. Keller, in *Proceedings of the 11th Conference on Ultrafast Phenomena*, T. Elsaesser, J. G. Fujimoto, D. A. Wiersma, and W. Zinth, eds., Vol. 63 of Springer Series in Chemical Physics (Springer, New York, 1998), p. 13.
6. A. Rundquist, C. Durfee, Z. Chang, G. Taft, E. Zeek, S. Backus, M. M. Murnane, H. C. Kapteyn, I. Christov, and V. Stoev, Appl. Phys. B **65,** 161 (1997).
7. A. Baltuška, Z. Wei, M. S. Pshenichnikov, D. A. Wiersma, and R. Szipöcs, Appl. Phys. B **65,** 175 (1997).
8. R. Trebino, K. W. DeLong, D. N. Fittinghoff, J. Sweetser, M. A. Krumbügel, and B. Richman, Rev. Sci. Instrum. **68,** 1 (1997).
9. G. Taft, A. Rundquist, M. M. Murnane, I. P. Christov, H. C. Kapteyn, K. W. DeLong, D. N. Fittinghoff, M. A. Krumbügel, J. N. Sweetser, and R. Trebino, IEEE J. Sel. Topics Quantum Electron. **2,** 575 (1996).
10. A. Baltuška, M. S. Pshenichnikov, and D. A. Wiersma, Opt. Lett. **23,** 1474 (1998).
11. M. Nisoli, S. De Silvestri, O. Svelto, R. Szipöcs, K. Ferenz, C. Spielmann, S. Sartania, and F. Krausz, Opt. Lett. **22,** 522 (1997).
12. U. Morgner, F. X. Kärtner, S. H. Cho, Y. Chen, H. A. Haus, J. G. Fujimoto, E. P. Ippen, V. Scheurer, G. Angelow, and T. Tschudi, Opt. Lett. **23,** 411 (1999).